Defence Science Journal, Vol. 68, No. 5, September 2018, pp. 480-486, DOI : 10.14429/dsj.68.12078

Range Performance Modelling of Thermal Imaging System based on Single Parameter Characterised by Ambient Temperature and Relative Humidity

Sudhir Khare[#,*], Manvendra Singh[#], and Brajesh Kumar Kaushik[@]

[#]*DRDO-Instruments Research and Development Establishment, Dehradun - 248 008, India*
[@]*Indian Institute of Technology, Roorkee - 247 667, India*
[*]*E-mail: sudhir_khare@hotmail.com*

ABSTRACT

Range performance of a thermal imaging system is characterised by the prevailing atmospheric condition present at that time. There are two dominant parameters that limit the range performance of any thermal imaging systems i.e. ambient temperature and relative humidity. In the present work, comparative study of acquisition range performance of thermal imaging system operating in the long wavelength infrared (LWIR) and medium wavelength infrared (MWIR) and spectral bands has been presented as a function of absolute humidity (AH) which is responsible for attenuation of IR radiation due to water vapour molecules present in path length. Presentation of acquisition range as function of AH leads to a single range performance table/graph for thermal imaging system under consideration for predefined visibility, target size, ambient temperature, target to background temperature difference and relative humidity. This table/graph can be used to predict detection, recognition and identification ranges for any set of combination of air temperature and relative humidity. The approach presented in this paper is versatile and has been illustrated through comparative performance analysis of LWIR and MWIR thermal imaging systems based on 640 x 512 staring focal plane array having identical design parameters in terms of resolution. It has been shown that MWIR performance is superior to LWIR beyond a crossover value of AH(T) even though MRTD of MWIR sensor is inferior to that of LWIR sensor at all spatial frequencies. Study has been carried out both for clear atmosphere and hazy conditions.

Keywords: Thermal imaging; Long wavelength infrared; Medium wavelength infrared; Atmospheric transmission; Acquisition range; Absolute humidity

1. INTRODUCTION

Thermal imaging system for terrestrial surveillance applications have been limited to 3-5 µm (Medium wavelength infrared (MWIR)) and 8-12 µm (long wavelength infrared (LWIR) spectral bands due to absorption effects produced by atmosphere. The performance of imaging systems operating in MWIR and LWIR bands[1] differ under prevailing atmospheric conditions such as ambient temperature, relative humidity, target signature, target to background temperature difference (ΔT) and operating path length. Therefore, it is mandatory to analyse and compare the range performance of these MWIR and LWIR imaging systems. It helps the designer to model the system parameters prior to develop and evaluate their range performance. The parametric characterisation ensures that the predicted ranges are close to the practical ranges achieved during field evaluation. In present paper, the performance comparison of MWIR and LWIR imaging systems has been presented. In order to have meaningful evaluation, IR detectors with identical FPA array, size and pixel pitch have been considered. Signal characteristics and design parameters of both the systems are same in terms of resolution (IFOV). LWIR and MWIR detectors having 640 x 512 staring focal plane array (FPA) and pixel pitch of 15 µm are considered for comparative analysis.

To predict the range performance, huge amount of data under varying ambient temperature (*T*), relative humidity (*RH*) and predefined visibility is required. It becomes impractical to quickly estimate the range performance for desired set of parameters. In the present work, single parameter i.e. Absolute humidity (*AH*) is used to evaluate the thermal sight range performance, as it takes into account the attenuation due to water vapour molecules characterised by *T* and *RH*. Acquisition range prediction methodology presented in this paper provides a single table/graph of thermal sight for specific target size, Δ*T* and discrimination task. It is much more user friendly and gives better insight into combination of *T* and *RH* which result in the same acquisition range.

2. MRTD AS A FIGURE OF MERIT FOR ESTIMATION OF ACQUISITION RANGES

Minimum resolvable temperature difference (MRTD)[2-4] gives the subjective resolving capability of device-observer system and is defined as the minimum target to background temperature difference in a vertical four bar pattern[5] of 7:1 aspect ratio which can just be resolved by an observer viewing the target through the sensor. MRTD is a measurable figure of merit as a function of spatial frequency which includes all the major image quality parameters including system modulation

Received : 10 September 2017, Revised : 29 July 2018
Accepted : 31 July 2018, Online published : 12 September 2018

transfer function (MTF) and noise equivalent temperature Difference (NETD). Typically, the MRTD[3,4] is given by:

$$(MRTD)_x = \frac{1.91 NETD}{(MTF)_x \sqrt{\tau_e}\sqrt{F_R}} \quad (1)$$

where F_R is frame rate and τ_e is eye integration time. $(MRTD)_x$ indicates the value of MRTD in horizontal direction and $(MRTD)_y$ indicates the value of MRTD in vertical direction.

The *NETD*[1,6,7] is given by:

$$NETD = \frac{4(F\#)^2.(\Delta f)^{1/2}}{\sqrt{xy}.\int_{\lambda_1}^{\lambda_2} D^*(\lambda)\frac{dN(\lambda)}{dT}d\lambda.\tau_o.\tau_a} \quad (2)$$

where

F#	f-number
x,y	Detector pitch
$\frac{dN(\lambda)}{dT}$	Spectral radiance contrast
D^*	Peak detectivity
τ_0	Optics transmittance
τ_a	Atmospheric transmittance
Δf	Noise equivalent bandwidth ($\Delta f \propto 1/t_{int}$)
t_{int}	Integration time

The thermal imaging system being linear shift invariant, the overall system MTF is defined as the product of system components MTF's of system components[8,9]

$$(MTF)_S = MTF_{opt}(f)\times MTF_{det}(f)\times MTF_{elec}(f)\times MTF_{disp}(f)\times MTF_{eye}(f)\times MTF_{atmosphere}(f) \quad (3)$$

3. ABSOLUTE HUMIDITY

Mass of water vapour in gm m^{-3} contained in saturated air for different temperatures can be derived from Eqn. (15-7) of reference[10], and is referenced as follows

$$AH = 1322.8\frac{RH}{T}.\exp\left[\frac{25.22(T-273.16)}{T} - 5.31\ \ln\left(\frac{T}{273.16}\right)\right] \quad (4)$$

where *RH* is the relative humidity, *AH* is absolute humidity (gm m^{-3}), and *T* is the temperature in Kelvin. Equation (4) can be rewritten as

$$AH = k(T) \times RH \quad (5)$$

where $k(T)$ represents the equivalent liquid H_2O content in gm m^{-3} in saturated air at temperature *T* in °C, *RH* is the relative humidity and *AH* is a measure of equivalent liquid H_2O content for $0.0 \le RH \le 1.0$ in air at temperature *T*. Values of $k(T)$ for limited temperature range have been listed in Table 1[10] for ready reference. For given *AH*, possible combinations of *T* and *RH* can be obtained first by reading the value of *k(T)* for desired *T* using Table 1 for $k(T) \ge AH$ and next using Eqn.(5) to determine *RH*(as a fraction). On the other hand if *T* and *RH* are specified, *AH* can be determined by first reading off the value of $k(T)$ corresponding to *T* from Table 1 and next multiplying $k(T)$ by *RH* (as a fraction). For example, $T = 15$°C and $RH = 63$ per cent, $k(T)$ is 12.7 from Table 1 and from Eqn. (5), $AH(T) = 8$.

4. ACQUISITION RANGE PREDICTION

Performance of a any thermal imager (TI)[11,12] is normally specified in terms of its minimum resolvable temperature difference (MRTD)[2-4] which is function of spatial frequency in cy/mrad. An apparent temperature differential ΔT_c at sensor end is given by Beer-Lambert (or Beer's law) law[10]:

$$\Delta T_c = \tau_a(R)\times \Delta T \quad (6)$$

where ΔT is temperature differential between target to background and $\tau_a(R)$ is the atmospheric transmission[7] for path length *R* which is given by

$$\tau_a(R) = e^{-ab.R}\times e^{-sc.R} \quad (7)$$

where *ab* is the atmospheric absorption coefficient and *sc* is the scattering coefficient

In order of concentration (by percent of volume), the gases in a dry atmosphere are Nitrogen, Oxygen, Argon, Neon, Helium, Krypton, Xenon, Hydrogen, Nitrous Oxide and trace gases. The gases present in variable amounts are Ozone, water vapour, Carbon Dioxide, Carbon Monoxide and other trace gases. Aerosols (suspended particles) include dust, dirt, carbon, minute organisms, sea salt, water droplets (haze or fog), smoke and artificial aerosols (pollutants). However, atmosphere is continuously changing and the constituents vary hourly, daily seasonally and by location etc. It is therefore not possible to assign a single number to the transmittance. These values must be measured or at least estimated at regular intervals when performing measurement or any specific activity.

System MRTD curves gives the maximum resolvable spatial frequency f_c corresponding to input ΔT_c.

Range equation[10,12] is given by

$$\frac{H}{R}.f_c = N \quad (8)$$

where *H* is height of target, *R* is acquisition range and *N* is the number of resolvable cycles. Johnsons criteria[10] for 50% probability of detection ($N=1$), recognition ($N=4$) and identification *(N=8)* is then used to predict the range performance of thermal imager.

5. ATMOSPHERE MODELLING: MODTRAN

In the present analysis atmospheric transmittance

Table 1. Mass of water vapour in saturated air, gm m^{-3}

Temp (°C)	0	1	2	3	4	5	6	7	8	9
0	4.84	5.18	5.54	5.92	6.33	6.76	7.22	7.70	8.22	8.76
10	9.33	9.94	10.57	11.25	11.96	12.71	13.50	14.34	15.22	16.14
20	17.22	18.14	19.22	20.36	21.55	22.80	24.11	25.49	27.0	28.45
30	30.04	31.70	33.45	35.28	37.19	39.19	41.7	43.91	46.22	48.64
40	51.16	53.79	56.53	59.40	62.38	65.50				

calculations have been carried out using latest model moderate resolution transmission (MODTRAN)[13] developed by Spectral Sciences, Inc. (SSI) and the US Air Force Research Laboratory (AFRL) because of its composite structure and adaptability. MODTRAN offers two general ways to define atmospheric parameters. The user can either enter meteorological data or use one of the atmospheric generic model. Standard atmospheres model contain a 34 layer atmosphere, with 1 km thick layers from 0-25 km altitude, 5 km thick layers from 25 km - 50 km altitude, and two layers covering 70 km and 100 km. According to season and latitude, the five generic profiles are as under:

(i) Tropical (15^0 North)
(ii) Mid-latitude summer (45^0 North, July)
(iii) Mid-latitude winter (45^0 North, January)
(iv) Sub-arctic summer (60^0 North, July)
(v) Sub-arctic winter (60^0 North, January)

These five models intend to represent average seasonal and latitude variations in atmospheric properties. The three parameters that exhibit the most significant changes with location and time are the atmospheric pressure, temperature and water concentration. All other constituent molecules are relatively uniformly distributed around the globe.

The atmospheric transmittance studies have been carried out in 3-5 μm and 8-12 μm spectral bands taking following parameters into consideration:

(a) Atmospheric profiles: Tropical (T) (15 degrees North), mid-latitude summer (45^0 North, July) and mid-latitude winter (45^0 North, January). Atmospheric profiles have been considered as India ($8^o4'$ N to $37^o6'$ N) lies in this region
(b) Visibility : 23 km (clear visibility) and 5 km (Haze)
(c) Water vapour

Table 2 presents the temperature and relative humidity at varying altitudes for tropical atmospheric profiles as per the MODTRAN atmospheres. These data are useful for providing typical reasonable values for average atmospheric conditions.

6. LWIR AND MWIR SYSTEM DESIGN PARAMETERS

Factors affecting the acquisition range performance of sensors in LWIR and MWIR[14] regions of spectrum are generally well known. LWIR (8-12 μm) band has higher thermal derivative and higher radiance, the MWIR (3-5 μm) offers higher relative contrast. Traditional thermal imagers have shown limited performance in MWIR (3-5 μm) spectral band due to the low radiance, particularly at low background temperatures. Recent advances in 3-5 μm sensor technology have overcome these limitations. Table 3 indicates the weightage, which can be assigned to different parameters in MWIR and LWIR bands.

Peak D:* Theoretical value of D* at the spectral peak for background limited photon (BLIP) detector is minimum at 14 μm at background temperature of 300°K and increases rapidly as wavelength is decreased below 14 μm[5] . In present analysis, as per manufacturer's data sheet the value of D*(Peak) in MWIR is taken to be higher by a factor of 5 as compared to LWIR.

Radiation Contrast: Differential radiance $\Delta N = \int_{\lambda_1}^{\lambda_2} \frac{dN(\lambda)}{dT} d\lambda$ in LWIR (7.7 μm - 10.5 μm) is higher approximately by a factor of 10 as compared to MWIR (3.6 μm - 4.9 μm) region for background temperature of 300° K. The parameter weighs heavily in favour of LWIR band.

Optics MTF: For the sake of simplicity, diffraction limited optical system has been considered for both the systems. Optics MTF $T_{opt}(f)$ is obviously higher in MWIR region at all spatial frequencies as compared to LWIR because cut-off frequency for MWIR system is 62.5 cycles/mm as compared to 43.5 cycles/mm for LWIR system in the selected configuration.

Atmospheric Attenuation Due to Scattering: Due to wavelength dependant nature of scattering losses, LWIR region marginally scores over the MWIR region. In the Night Vision Laboratory (NVL) program for acquisition range prediction,

Table 2. Pressure, temperature and relative humidity at different altitudes for tropical atmospheric profiles

Altitude (Km)	Tropical atmosphere profile			Mid-latitude summer atmosphere profile			Mid-latitude winter atmosphere profile		
	Pressure (mbar)	Temp (K)	RH (per cent)	Pressure (mbar)	Temp. (K)	RH (per cent)	Pressure (mbar)	Temp (K)	RH (per cent)
0	1013.0	299.7	75.53	1013.0	294.2	76.11	1018.0	272.2	77.0
1	904.0	293.7	72.77	902.0	289.7	65.97	897.3	268.7	70.44
2	805.0	287.7	74.51	802.0	285.2	55.15	789.7	265.2	65.40
3	715.0	283.7	48.25	710.0	279.2	45.26	693.0	261.7	56.69
4	633.0	277.0	34.91	628.0	273.2	39.02	608.1	255.7	49.85
5	559.0	270.3	37.71	554.0	267.2	31.39	531.3	249.7	47.13
6	492.0	263.6	34.79	487.0	261.2	29.96	462.7	243.7	43.98
7	432.0	257.0	31.98	426.0	254.7	30.29	401.6	237.7	31.01
8	378.0	250.3	29.47	372.0	248.2	29.61	347.3	231.7	23.0
9	329.0	243.6	25.35	324.0	241.7	30.13	299.3	225.7	19.65
10	286.0	237.0	19.51	281.0	235.3	29.42	256.8	219.7	17.91

Table 3. Comparative performance 3-5 µm and 8-12 µm spectral band

Parameters	3-5 µm	8-12 µm
Integrated photon flux	Lower	150 times more
Radiation contrast	Lower	Higher
Relative contrast	Higher (Better S/N)	Lower S/N
Peak D*	Higher	Lower
NETD for a fixed system	Lower	Higher
Atmospheric transmission	Better in marine environment	
Transmission through dust and fog	--	Better
Transmission in hot and humid environment	Better	--
Ranges	Better for long ranges >6Km	Better for ranges<6Km
Cost	Lower	Higher

aerosol scattering is taken into account by the user defined parameter V (visibility).

Atmospheric Attenuation Due to Absorption: Absorption of IR radiation in the atmospheric path between the target and the sensor is primarily due to water vapour molecules and CO_2 molecules (4.2 µm to 4.4 µm in MWIR). Attenuation due to water vapour molecules is characterised by two user defined and measurable parameters viz. ambient temperature *T* and relative humidity *RH*. Usual approach for predicting acquisition range performance of thermal sight is to use the NV Therm-IP model developed by Night Vision and Electronic Sensors Directorate's (NVESD), US Army to generate set of tables or graphs for desired values of *T* and *RH* for predefined visibility *V*.

LWIR and MWIR Sensor Design Parameters

Systems under consideration are thermal imagers[15] based on LWIR 640 x 512 and MWIR 640 X 512 detectors. Design parameters of LWIR and MWIR thermal imager[14] are listed as follows

(i) LWIR Thermal Imager Parameters

Spectral band	7.7 µm – 10.5 µm
Detector	640 x 512 FPA, 15 µm pitch
Peak D*	1.0 x 10^{11} cmHz$^{1/2}$W^{-1}
Optics	110 mm dia, f/2.7
EFL	297 mm
IFOV	50 µrad
FOV	1.8° x 1.4° (NFOV)
Wavelength for diffraction	8.5 µm
Optical transmission	0.8
Display	CRT (spot size 0.01 mm^2)

(ii) MWIR Thermal Imager Parameters

Spectral band	3.6 µm – 4.9 µm
Detector	640 x 512 FPA, 15 µm pitch
Peak D*	5.0 x 10^{11} cm Hz$^{1/2}$ W^{-1}
Optics	75 mm dia, f/4
EFL	300 mm
IFOV	50 µrad
FOV	1.8° x 1.4° (NFOV)
Wavelength for diffraction	4.25 µm
Optical transmission	0.8
Display	CRT (spot size 0.01 mm^2)

7. RESULTS AND DISCUSSIONS

For the LWIR and MWIR sensors described in section-6, the horizontal MRTD as function of spatial frequency in cycles/mrad has been presented in Fig. 1. The MRTD[16-18] takes into account the spectral band dependant parameters viz. peak *D**, radiation contrast and the optics *MTF*. It may be seen from Fig. 1 that LWIR sensor has lower MRT values as compared to MWIR sensor at all spatial frequencies. In other words, as far as the sensor is concerned, the LWIR is superior to MWIR even though the design parameters and detector topology are identical for the two sensors. Night vision thermal and image processing performance model (NVTHERM-IP) developed by NVESD, US Army[17] have been used for acquisition range calculations.

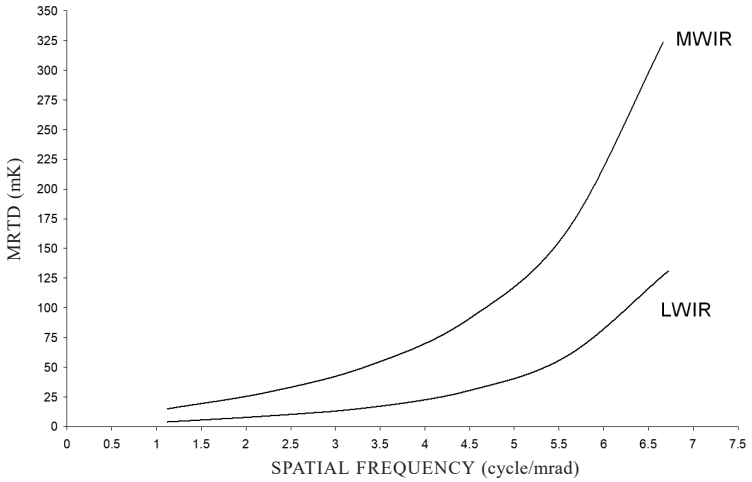

Figure 1. Horizontal MRTD for the MWIR and LWIR sensors as function of spatial frequency.

Comparative detection, recognition and identification range performance[19-21] for the two thermal imaging systems against a standard NATO target of size 2.3 m x 2.3 m with ΔT = 2 °C for clear atmosphere characterised by *V*=23 km and haze characterised by 5 km have been given as function of *AH* in Fig. 2 to 4.

For clear atmosphere characterised by *V*=23 km, the detection, recognition and identification ranges are plotted with respect to different atmospheric conditions. Two extreme conditions of *AH* are considered. In the first case, where *AH*=4 (*T*=5 °C, *RH*=60 per cent), detection, recognition and identification ranges in LWIR and MWIR are comparable. Detection ranges are 16.6 km and 16.0 km; Recognition ranges, 5.1 km and 4.8 km; and identification ranges, 4.1 km and 3.8 km, respectively. For relatively hot and humid conditions pertaining to *AH* = 40 (*T*=40° *C, RH*=80 per cent), detection, recognition and identification ranges in LWIR and MWIR differ substantially. Detection ranges are 3.7 Km and 12.3 km; Recognition ranges; 2.1 km and 4.1 km; and identification ranges; 1.8 Km and 3.5 km, respectively in the two bands.

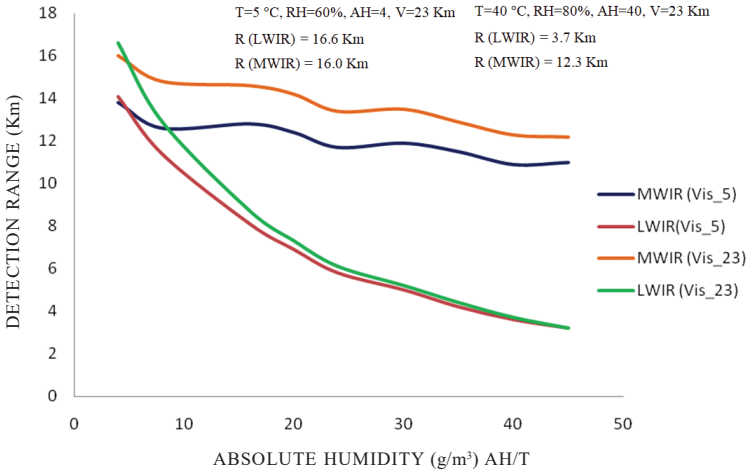

Figure 2. Detection range for MWIR/LWIR sensors as function of AH(T) for V = 23 km and V = 5 km against 2.3 m x 2.3 m target with ΔT = 2 °C.

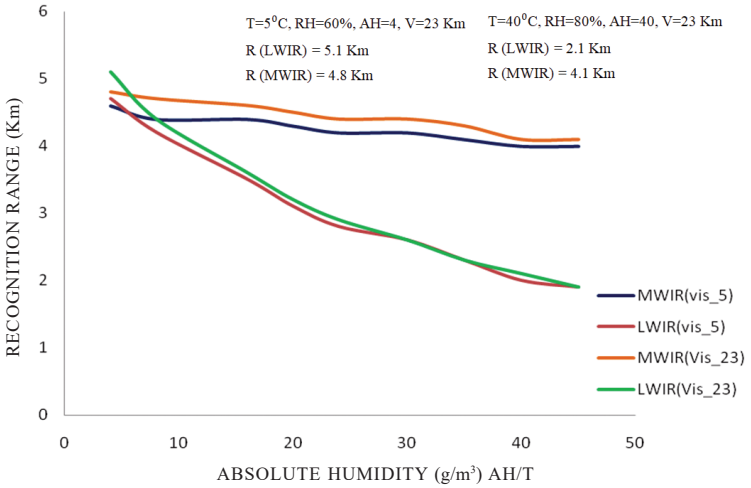

Figure 3. Recognition range for MWIR/LWIR sensors as function of AH(T) for V=23 km and V = 5 km against 2.3 m x 2.3 m target with ΔT = 2 °C.

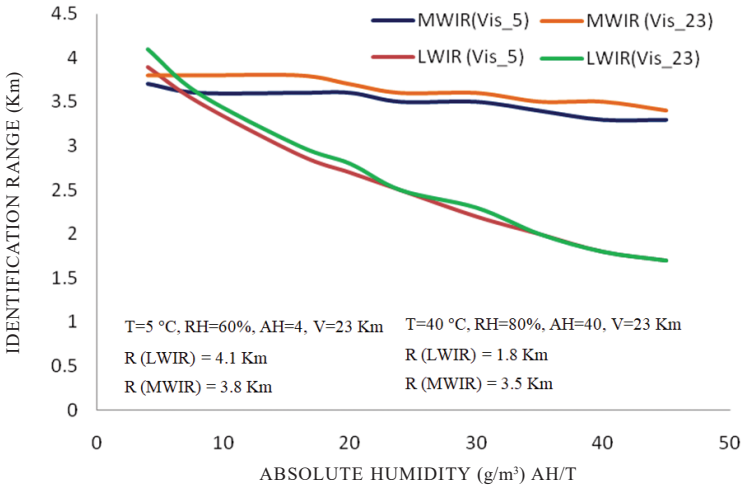

Figure 4. Identification range for MWIR/LWIR sensors as function of AH(T) for V=23 km and V = 5 km against 2.3 m x 2.3 m target with ΔT = 2 °C.

There is wide gap in the ranges of two wavebands. LWIR performance is drastically going down as compared to MWIR in hot and humid regions.

In general as evident from Figs. 2, 3, and 4, there is little effect of increasing $AH(T)$ on acquisition range in MWIR region whereas there is drastic reduction in LWIR region. An interesting observation that can be made is that there is a crossover point near $AH(T) = 6$ beyond which MWIR sensor scores over LWIR sensor as far as range performance is concerned even though the MWIR sensor is inferior to its LWIR counterpart in terms of performance parameter MRTD.

Next we consider atmospheric condition characterised by HAZE for visibility V=5.0 km, even under hazy conditions, same trends have been observed and the crossover point shifts only slightly from $AH(T) = 6$. Effect of haze on the acquisition range of LWIR sensor is negligible. For the MWIR sensor, percentage drop in detection range is around 13 per cent. In other words, effect of aerosol scattering on MWIR acquisition range is more significant than absorption.

8. VALIDATION OF RANGES AND ANALYSIS

Validation trials at sea shore and desert environment have been carried out with following similar thermal imagers:

Parameter/ camera	Thermal imager-I	Thermal imager-II
Spectral range	8-10.5 µm (LWIR)	3-5 µm (MWIR)
WFOV	6.0° X 4.5°	8.8° X 6.4°
NFOV	2.0° X 1.5°	2.2° X 1.6°

It was observed during trial, the range performances of 3-5 µm thermal imager performed better than 8-12 µm in marine environment at high AH (same is achieved using range performance modelling shown in Table 4). For AFV application (desert environment) also, same results have been achieved at high AH, however, at lower AH from 4-6, LWIR thermal imager scores over MWIR thermal imager as shown in Table 4. The target at 8.5 km was getting merged with the background in 8-12 µm thermal imager while the same target could be recognised distinctly in 3-5 µm camera. The thermal image captured during trials is as shown in Fig. 5.

9. CONCLUSIONS

Comparative performance analysis and predicting acquisition ranges of LWIR and MWIR thermal imager is a complex task. It is known that choice between LWIR and MWIR bands depends upon various target characteristics and environmental factors such as target size, T, RH and ΔT. In the present work, prediction of range performance based on single parameter i.e. Absolute humidity (AH) is presented. The results obtained through range modelling are very close to the ranges achieved practically during field trials. The proposed single parameter based range

Table 4. Recognition ranges achieved in sea and desert environment

Target size	RH (%)	T (°C)	AH	Visibility (Km)	Predicted recognition range (Km)	Achieved recognition range (Km)
Tank (2.3m x 2.3m)	45	11-15	4-6	15	5.2 4.8	5.0 NFOV(8-12 µm) 4.7 NFOV(3-5 µm)
Tank (2.3m x 2.3m)	25	42-45	14-16	15	3.2 4.5	3.6 NFOV(8-12 µm) 4.7 NFOV(3-5 µm)
Tank (2.3m x 2.3m)	76	28-30	20-22	15	2.8 4.5	2.8 NFOV(8-12 µm) 4.5 NFOV(3-5 µm)
Merchant ship (L≈130m)	68-73	34-36	25-30	15-18	--	7.5 NFOV(8-12 µm) 17.0 NFOV(3-5 µm)
Cargo ship (L≈110m)	73-80	36-38	30-37	10-12	--	3.5 NFOV(8-12 µm) 13.0 NFOV(3-5 µm)

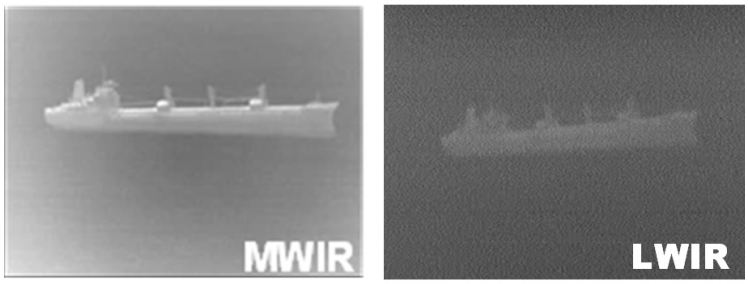

Figure 5. Image captured by MWIR and LWIR thermal imager.

prediction method results quick performance evaluation which reduces the efforts of collection of huge data having varied *T* and *RH* and also reduces the computational efforts required on analysing the huge data set.

It has been shown that atmospheric transmission in MWIR and LWIR band is highly dependent on *T* and *RH* in terrestrial scenario and there exists a crossover point in terms of absolute humidity beyond which MWIR acquisition range is higher than that of LWIR. Atmospheric transmission decreases with increasing value of absolute humidity (*AH*) in MWIR and LWIR band due to water vapour molecules. Also, the effect of increased temperature and humidity is less evident in MWIR region as compared to LWIR region. For shorter ranges upto 5-6 km, LWIR scores over MWIR thermal imager. But in hot and humid conditions, MWIR system performs extremely well in detection, recognition and identification ranges. For the Indian army where the battle-field conditions vary from hot and humid conditions of Rann-of-Kutch to snow-clad areas in the Himalayas, it is recommended to use both LWIR and MWIR sensors. However, for naval applications where the ambient conditions are around 30 °C and 85 per cent *RH* throughout the year, the MWIR sensor is a clear choice.

REFERENCES

1. Burdette, E. M.; Teague, J.R.; Dobbins, C.L. & Wood, S.B. Comparative performance of large format MWIR and LWIR Systems in NV-IPM. *In* Proceedings of SPIE 9452, 2015, pp. 94520O-1 to O-9.
2. Lloyd, J.M. Thermal imaging systems. *In* Plenum Press, New York, 1975, pp. 166-21.
3. Hudson, R.D. Infrared system engineering. *In* John Wiley & Sons, NY, 1969.
4. Burks, S.D.; Doe, J.M. & Teaney, B.P. Validating machine vision MRT performance against trained observer performance for linear shift invariant sensors. *In* Proceedings of SPIE 9452, 2015, pp. 945204-1 - 8. doi: 10.1117/12.2178149.
5. Han, Shun-li; Zhang, Peng & Hu, Wei-liang. Infrared simulation of 4-bar target for the static performance evaluation of thermal imaging system. *In* Proceedings of SPIE 8912, 2013, pp. 891204-1 to 7. doi: 10.1117/12.2031663.
6. Norton, P.; Understanding the NEΔT of tactical infrared focal plane arrays. *J. Opto-electr. Rev.*, 2012, **20**(3), 275-278.
7. Preece, B; Hodgkin, V.A.; Thompson, R.; Leonard, K. & Krapels, K. Predicted NETD performance of polarised infrared imaging sensor. *In* Proceedings of SPIE 9071, 2014, pp. 90710C-1 to C-10. doi: 10.1117/12.2052960.
8. Hixson, J.G.; Haefner, D.P. & Teaney, B. Comparing and contrasting different broadband MTF definitions and the relationship to range performance prediction. *In* Proceedings of SPIE 9071, 2014, pp. 907105-1 to 8. doi: 10.1117/12.2050362.
9. Kaur, B; Olson, J. & Flug, E.A. Display MTF measurement based on scanning and imaging technologies and its importance in the application space. *In* Proceedings of SPIE 9820, 2016, pp. 98200Y-1 to Y-11. doi: 10.1117/12.2223960.
10. Holst, G.C. Electro-optical imaging system performance. *In* JCD Publishing, Third Edition, Florida, SPIE Optical Engineering Press, Bellingham, Washington, 2003, pp. 355-384.
11. Chensheng, Wang; Xiaodong, Guo; Tingting, Ren & Zhijie, Zhang. Performance evaluation of infrared imaging system in field test. *In* Proceedings of SPIE 9300, 2014, pp. 93002J-1 to 7, doi: 10.1117/12.2074332.
12. Teaney, B.P.; Tomkinson, D.M. & Hixon, J.G. Legacy modeling and range prediction comparision: NV-IPM versus SScamIP and NVTHERM. *In* Proceedings of SPIE 9452, 2015, pp. 94520P-1 to P-12, doi: 10.1117/12.2179371.
13. Dylan, Payne & John, Schroeder. Sensor performance

and atmospheric effects using NVThermIP/ NV-IPM and PcModWin/ MODTRAN models- a historical perspective. *In* Proceedings of SPIE 8706, 2013, pp. 87060G-1 to 13. doi: 10.1117/12.2016101.

14. Seán, M. Stewart. Analysis of the relative merits of the 3-5 μm and the 8-12 μm spectral bands using detected thermal contrast. *In* Proceedings of SPIE 9485 on Thermal Infrared Applications XXXVII, 2015, doi: 10.1117/12.2176940.
15. Szajewska, A. Development of thermal imaging camera (TIC) technology. *In* Proceedings of ELSEVIER: Procedia Engineering on Modern Building Materials and technologies MBMST. 2017, pp. 1067-1072.
16. Yi-chin & Bo-Wen, Wu. Prediction of thermal imaging minimum resolvable (circle) temperature difference. *IEEE Trans. Pattern Anal. Mach. Intelligence,* 2008, **30**(12), 2218-2228.
17. Night Vision Thermal and Image Processing Performance Model, User's Manual, Document: Rev 10, U.S. Army RDECOM CERDEC, Night Vision and Electronic Sensors Directorate, Modeling and Simulation Division, Fort Belvoir, Aug. 2009.
18. Furxhi, O.; Driggers, R.G.; Preece, B. & Krapels, K. Modeling analysis metrics for panoramic sensors. *In* Proceedings of SPIE 9452, 2015, pp 945209-1 to 12. doi: 10.1117/12.2179740.
19. Burks, S.D; Haefner, D.P.; Teaney, B.P. & Doe, J.M. Thermal system field performance predictions from laboratory and field measurements. *In* Proceedings of SPIE 9820, 2016, pp 98200U-1 to U-7. doi: 10.1117/12.2224054.
20. Stephen, D. Burks; David, P. Haefner & Doe, Joshua M. Electro-optical field performance validation in the presence of turbulence. *In* Proceedings of SPIE 10178 on Infrared Imaging Systems: Design, Analysis, Modeling, and Testing XXVIII, 2017. doi: 10.1117/12.2261390.
21. Gao, Jingli; Wen, Chenglin & Liu, Meiqin Robust small target co-detection from airborne infrared image sequences. *Journal of Sensors*, 2017, 2242.

CONTRIBUTORS

Mr Sudhir Khare is presently working as Scientist in DRDO-Instruments Research and Development Establishment, Dehradun. He has been engaged in research, design and development in the area of thermal imaging for last 25 year. His research interests include system design, IR signal processing and performance evaluation of thermal imaging systems. He has published more than 20 paper in journals and is also a Life Member of Optical Society of India. He is recipient of *DRDO scientist of the year award 2017* and *Agni Award for Excellence in Self Reliance in 2009, 2012 and 2014*.
In the Current study, he has carried out comparative acquisition range performance analysis of thermal imaging system operating in LWIR and MWIR spectral bands through mathematical model under varying atmospheric conditions.

Mr Manvendra Singh, obtained MTech (VLSI & Microelectronics) from IIT Kanpur, in 2002. Currently working as a Scientist DRDO-Instruments Research and Development Establishment, Dehradun. He has wide knowledge and experience of design and development of Electro-optical Instruments for fire control and stand-alone surveillance systems. He has published more than 15 paper in journals and is also a Life Member of Instruments Society of India. He is recipient of *DRDO scientist of the year award 2015.*
Contribution in the current study, he has carried out range performance validation of thermal imagers operating in LWIR and MWIR spectral bands in field ranges

Dr Brajesh Kumar Kaushik received PhD from Indian Institute of Technology, Roorkee, in 2007. Presently he is working as an Associate Professor at Department of Electronics and Communication Engineering, Indian Institute of Technology, Roorkee, India. His research interests are in the areas of high-speed interconnects, low-power VLSI design, memory design, carbon nanotube-based designs, organic electronics, FinFET device circuit co-design, electronic design automation (EDA), spintronics-based devices, circuits and computing, image processing, and optics and photonics based devices.
Contribution in the current study, he has guided and supervised the work presented in this paper.